CHAPTER 4

INITIAL AND BOUNDARY CONDITIONS

Because we are solving an initial boundary value problem, it is necessary to specify the field over a depth grid at some initial range to start the computational procedure. Surface and bottom boundary conditions need to be specified as well. Potentially, a number of propagation models such as ray tracing, normal mode theory or the fast field program can be used to generate the starting field. However, for many applications, it is sufficient to approximate the initial field by a Gaussian function [1]. This latter procedure is discussed in this chapter.

Since, in most applications to low-frequency sound propagation, the surface may be treated as a pressure-release boundary, the field will be assumed to vanish on the surface. Specifying the bottom boundary condition is considerably more difficult, especially when limited environmental data are available. We present two different treatments of the bottom boundary condition. First, a special treatment of bottom boundary conditions of the rigid type is presented. This boundary condition will permit us to later make comparisons between predictions of the implicit finite difference (IFD) model and the exact solution for propagation in a wedge-shaped ocean. We then develop the major contribution of this chapter: a direct incorporation of the interface conditions between media of differing sound speeds and densities into the IFD computational scheme.

4.1. THE INITIAL FIELD

In this section, we describe how the initial field is specified using a Gaussian function, and refer the reader to Tappert [1] for a detailed derivation of this procedure. To generate the initial field, the Gaussian function must asymptotically match the solution to the reduced wave equation for a point source. Let us hence consider a Gaussian beam, where

G_w = the beam width, measured from 3 dB downward on the main lobe,
W_s = average wavenumber

and

G_s = amplitude of the Gaussian beam function.

Then, the above parameters can be related by

$$G_s = \frac{1}{G_w}\sqrt{\frac{2}{W_s}}. \tag{4.1}$$

Also, let

Δz = mesh point in the depth direction

and

z_s = source depth relative to the surface boundary.

Our matching criterion requires

$$\mathrm{Re}(u_0) = G_s\left(\exp\left[-\left(\frac{\Delta z - z_s}{G_w}\right)^2\right] - \exp\left[-\left(\frac{-\Delta z - z_s}{G_w}\right)\right]^2\right). \tag{4.2}$$

The imaginary part $\mathrm{Im}(u_0)$ is set to zero.

4.2. A NEUMANN BOTTOM BOUNDARY CONDITION

A treatment of a homogeneous Neumann bottom boundary condition is discussed here. In general, the existence of an irregular bottom boundary profile, as shown in Fig. 4.1, is assumed. Given such a boundary, a piecewise linear line segmentation is then applied to describe the bottom profile.

This linearization process permits automatic handling of the bottom boundary, and also provides a systematic way of treating a sloping bottom. Assume the sloping boundary makes an angle Θ with the horizontal, then, the outward normal derivative operator is expressed by

$$\frac{\partial}{\partial z}\cos\Theta - \frac{\partial}{\partial r}\sin\Theta.$$

For the wave field of the reduced wave equation $p(r, z)$, the homogeneous Neumann bottom boundary condition requires that $p_N = 0$ on the boundary. Applying the normal derivative operator to the wave field $p(r, z)$, we obtain

$$\frac{\partial p}{\partial z}\cos\Theta - \frac{\partial p}{\partial r}\sin\Theta = 0. \tag{4.3}$$

Since

$$p(r, z) = H_0^{(1)}(k_0 r)u(r, z) = v(k_0\gamma)u(r, z), \tag{4.4}$$

substituting this expression into equation (4.3) gives

$$H_0^{(1)}(k_0 r)\frac{\partial u}{\partial z}\cos\Theta - (H_0^{(1)}(k_0 r))_r \sin\Theta\, u - H_0^{(1)}(k_0 r)\sin\Theta\, u_r = 0. \tag{4.5}$$

Since u_r satisfies the parabolic wave equation $u_r = a(k_0, r, z)u + b(k_0, r, z)u_{zz}$, equation (4.5) can be written as

$$H_0^{(1)}(k_0 r)\frac{\partial u}{\partial z}\cos\Theta - (H_0^{(1)}(k_0 r))_r \sin\Theta\, u - H_0^{(1)}(k_0 r)\sin\Theta\,(a(k_0, r, z)u + b(k_0, r, z)u_{zz}) = 0. \tag{4.6}$$

Upon rearranging the coefficients, equation (4.6) can be expressed in the form

$$u_{zz} + p_1 u_z + p_2 u = 0. \tag{4.7}$$

Equation (4.7) is a second order ordinary differential equation which can be treated as an initial value problem with

$$p_1 = -\cot\Theta / b(k_0, r, z), \tag{4.8}$$

$$p_2 = \left(\frac{(H_0^{(1)}(k_0 r))_r}{H_0^{(1)}(k_0 r)} + a(k_0, r, z)\right) \Big/ b(k_0, r, z), \tag{4.9}$$

and initial values for $u(r, z_B)$ and $\partial u/\partial z|_{z_B}$.

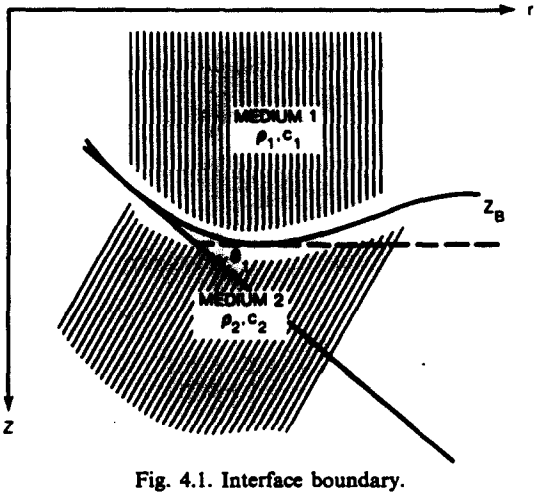

Fig. 4.1. Interface boundary.

Since the far-field approximation is valid, equation (4.9) can be further simplified. Recall that

$$H_0^{(1)}(k_0 r) = \sqrt{\frac{2}{\pi k_0 r}} \exp\left[i\left(k_0 r - \frac{\pi}{4}\right)\right],$$

then

$$(H_0^{(1)}(k_0 r))_r = \left[ik_0 - \frac{1}{2r}\right] H_0^{(1)}(k_0 r).$$

Therefore,

$$p_2 = \left[ik_0 - \frac{1}{2r} + a(k_0, r, z)\right] \Big/ b(k_0, r, z). \tag{4.10}$$

This special treatment is incorporated into the IFD model for application to rigid boundaries. Note that, for a horizontal Neumann boundary condition, the slope angle Θ is zero. A shallow-to-deep water case (Fig. 4.2) is used to illustrate the present treatment.

Our objective is to find u_m^{n+1} and then determine u_{m+1}^{n+1} to proceed with the matching scheme. Once u_{m+1}^{n+1} is found, we can proceed if we use proper care. Note that if the distance between u_m^{n+1} and u_{m+1}^{n+1} is not $= 2(\Delta z)$, we cannot proceed with the present method because the depth partition at this range level is not uniform. A special treatment is needed at some specific advanced range levels. To handle this, we label u_{m+1}^{n+1} as u_{m+2}^{n+1} and define u_{m+1}^{n+1} as the midpoint between u_m^{n+1} and u_{m+2}^{n+1}. We determine u_{m+1}^{n+1} in such a way that the distance between u_m^{n+1} and u_{m+2}^{n+1} is $2(\Delta z)$. This treatment ensures a uniform partition in the depth direction. The u_{m+1}^{n+1} can be found in the same way by solving equation (4.6).

A question arises: how far can we proceed in determining u_{m+1}^{n+1}? To ease the programming requirements and to maintain accuracy, we determine Δr by

$$\frac{\Delta z}{\Delta r} = \tan\alpha \rightarrow \Delta r = \Delta z \cdot \cot\alpha.$$

When we have proceeded Δr distance in range, it is time to determine u_{m+1}^{n+1}. For the deep-to-shallow case, as shown by Fig. 4.3, the treatment is the same as the shallow-to-deep water case. The only differences are α and Δz.

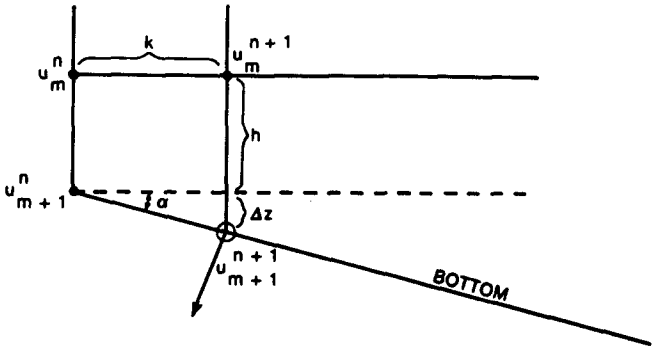

Fig. 4.2. Shallow-to-deep water case.

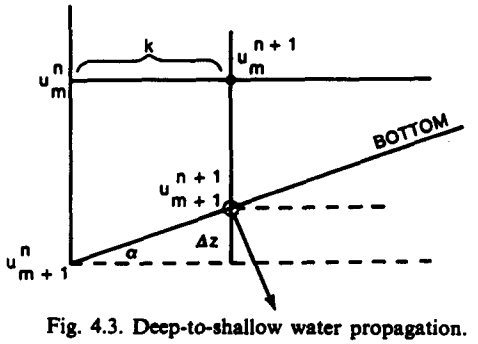

Fig. 4.3. Deep-to-shallow water propagation.

4.3. INTERFACE TREATMENT

In the ocean, temperature, salinity and pressure affect the sound-speed and density structure of the water mass creating a layered medium. The sediments that compose the ocean floor are also layered due to the periodic deposition of sedimentary material. These phenomena stratify the ocean environment into a layered medium, thus, forming interfaces. At each interface, "continuity conditions" hold; the pressure and normal component of particle velocity are continuous at the interface.

Many mathematical models exist to solve the wave equation in a *uniformly stratified* medium [2]. These models have been applied to demonstrate the sensitivity of acoustic propagation to the sound speed and density stratification of the seabed. In range-dependent environments, the propagated acoustic field may also be strongly dependent on bottom interaction, necessitating an accurate treatment of the field at the water sediment interface and at deeper interfaces within the seabed. In this section, a mathematical model of wave propagation in a range-dependent environment is developed that fully models the wave field at interfaces between media of differing sound speeds and densities.

Interface conditions applicable to the parabolic wave equation are derived that preserve both continuity of pressure and continuity of the component of particle velocity normal to the interface. These conditions, hence fulfill the necessary physical requirements. The case of an irregular interface is treated in general, results for the horizontal interface are hence included as a special case.

To obtain representations of the wave field on the interface, we use a method developed by Carnahan, *et al.* [3] to handle horizontal interface conditions (continuity of conductivity and diffusitivity) for the heat-transfer problem. Carnaham *et al.*'s basic approach is extended to treat irregular interface conditions for the parabolic wave equation. Specifically, a finite difference technique is used to match interface conditions at an irregular boundary between two different media. This procedure results in a finite difference approximation to the parabolic wave equation that holds on the interface. Moreover, this finite difference interface equation is compatible with an IFD solution [4] of the parabolic wave equation. To complete the formulation of our wave propagation model, the interface wave field representation is embedded in the IFD model. The validity of this mathematical model is then analyzed: the local truncation error is computed to establish that the model provides consistent parabolic equation (PE) solutions. Predictions are further compared with the results of other models to verify that the model provides an accurate treatment of the interface wave field.

We will obtain interface conditions for the standard parabolic wave equation

$$u_r = \frac{ik_0(n^2-1)}{2}u + \frac{i}{2k_0}u_{zz}, \tag{4.11}$$

This equation describes the transmitted field for wave propagation at small angles with respect to the horizontal, and is hence applicable to underwater sound propagation in many ocean environments. In the following sections, we develop a mathematical solution to the PE that accurately computes the wave field at interfaces.

4.3.1. Interface conditions

We treat the general case in which interfaces between physically distinct media in the ocean are *irregular* as shown in Fig. 4.4.

In Fig. 4.4, z_B indicates the interface depth, the density ρ of each medium is assumed constant, and the sound speed in each medium is a function of both range and depth. To develop systematic procedures for handling the irregular interface and to reduce mathematical difficulties in deriving the interface conditions, a piecewise linear segmentation is used to approximate the interface as shown in Fig. 4.5. We will, thus, obtain results for segments of the interface having a constant slope; the horizontal interface is then contained as a special case.

The pressure field in the ocean satisfies two conditions at an interface between two media. The first of these two conditions is the requirement that the pressure field be continuous at the interface

$$p_1(r, z_B) = p_2(r, z_B). \tag{4.12}$$

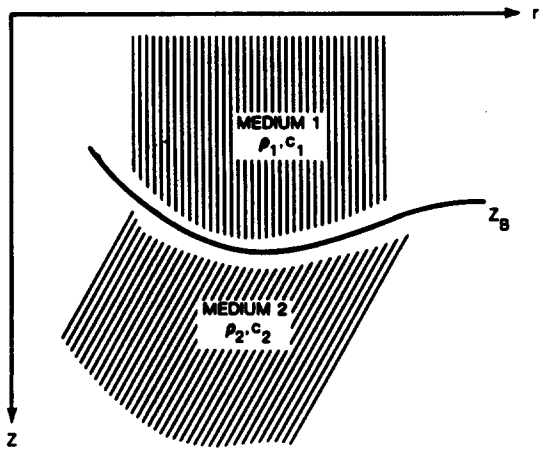

Fig. 4.4. An irregular interface.

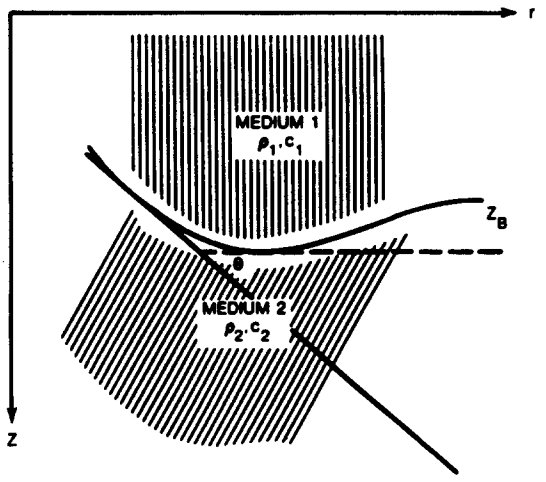

Fig. 4.5. Linear approximation of irregular interfaces.

The second interface condition is that the normal component of particle velocity be continuous at the interface, or that

$$\rho_2 \frac{\partial p_1}{\partial n}\bigg|_{z_B} = \rho_1 \frac{\partial p_2}{\partial n}\bigg|_{z_B}, \tag{4.13}$$

where $\partial/\partial n$ indicates the outward normal derivative operator. For the sloping interface, as shown in Fig. 4.6, the normal derivative operator is given by

$$\frac{\partial}{\partial n} = \cos\Theta \frac{\partial}{\partial z} - \sin\Theta \frac{\partial}{\partial r}. \tag{4.14}$$

If we now substitute equation (4.4) into equation (4.12), we obtain the first interface condition for the parabolic wave equation

$$u_1(r, z_B) = u_2(r, z_B). \tag{4.15}$$

To obtain the second interface condition, we substitute equation (4.4) into equation (4.13) and make use of equations (4.4) and (4.14). The result is

$$\rho_2\left[\frac{\partial u_1}{\partial z} v\cos\Theta - \frac{\partial u_1}{\partial r} v\sin\Theta\right]\bigg|_{z_B} - \rho_2 u_1 \frac{\partial v}{\partial r}\sin\Theta\bigg|_{z_B}$$

$$= \rho_1\left[\frac{\partial u_2}{\partial z} v\cos\Theta - \frac{\partial u_2}{\partial r} v\sin\Theta\right]\bigg|_{z_B} - \rho_1 u_2 \frac{\partial v}{\partial r}\sin\Theta\bigg|_{z_B}. \tag{4.16}$$

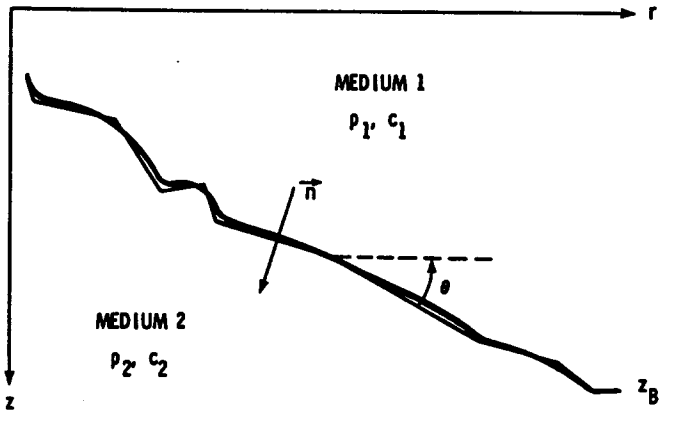

Fig. 4.6. A sloping interface and outward normal derivative.

The two conditions given by equations (4.15) and (4.16) hold for an interface of arbitrary slope. For the special case of a horizontal interface, $\Theta = 0$, equation (4.15) remains unchanged, equation (4.16), however, simplifies considerably reducing to

$$\rho_2 \frac{\partial u_1}{\partial z}\bigg|_{z_B} = \rho_1 \frac{\partial u_2}{\partial z}\bigg|_{z_B}. \tag{4.17}$$

4.3.2. Mathematical formulation of the wave field on the interface

To formulate finite difference equations for the wave field on the interface, we will use a mesh having a uniform partition in the z direction with $\Delta z = h$. The range is partitioned in increments $\Delta r = k$, as is shown in Fig. 4.7. At each mesh point, superscripts are used to indicate the range level; subscripts indicate the depth level. The wave field at the point (nk, mh) is written as u_m^n which also denotes the field on the interface. For economy in writing, we use the convention that if both the superscript and subscript are dropped, the field u means u_m^n.

We assume that u_j^n is known, and proceed to determine u_j^{n+i} for every i and j such that the interface conditions (4.15) and (4.16) are satisfied. Let us first write the parabolic wave equation in a general form

$$u_r = a(k_0, r, z)u + b(k_0, r, z)u_{zz}, \tag{4.18}$$

where

$$a(k_0, r, z) = \tfrac{1}{2} ik_0[n^2(r, z) - 1]$$

and

$$b(k_0, r, z) = i/(2k_0).$$

From here on in this chapter, if we deal with a flat interface, for economy in writing we omit the subscript; otherwise the subscript will be used properly to indicate the appropriate medium where $(m - 1)$ indicates medium 1, $(m + 1)$ indicates medium 2.

Medium 1

In medium 1, the wave field must satisfy equation (4.18), i.e.

$$(u_1)_r = a_1(k_0, r, z)u_1 + b_1(k_0, r, z)(u_1)_{zz}. \tag{4.19}$$

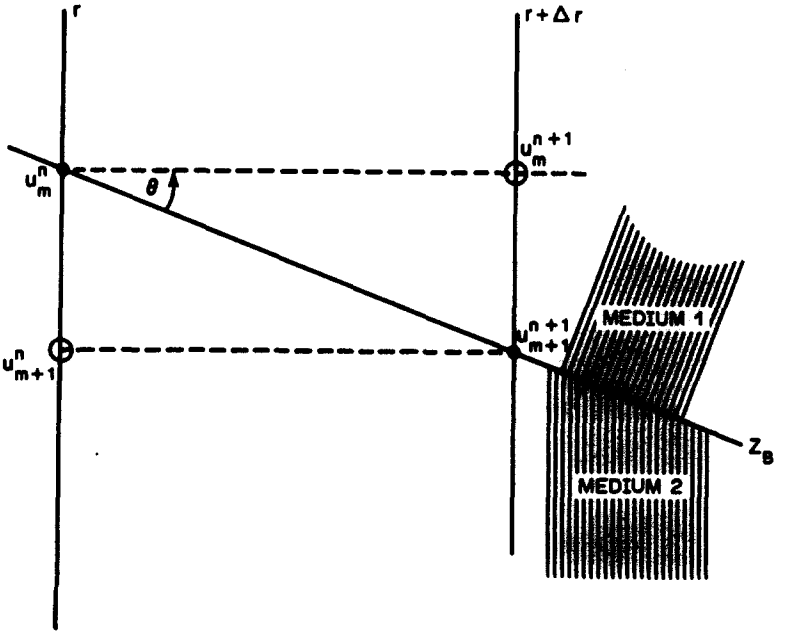

Fig. 4.7. The downward sloping interface between two media.

Using the first three terms of a Taylor series expansion for u_{m-1} upon u_m, and solving for $(u_1)_{zz}$, we find

$$(u_1)_{zz} = -\frac{2}{h^2}(u_1 - (u_1)^n_{m-1}) + \frac{2}{h}(u_1)_z. \tag{4.20}$$

Substituting equation (4.20) into equation (4.19) and simplifying, we obtain

$$(u_1)_z = \frac{h}{2b}(u_1)_r - \frac{h}{2b}a_1 u_1 + \frac{1}{h}(u_1 - (u_1)^n_{m-1}). \tag{4.21}$$

Medium 2

Similarly, in medium 2, the wave field must satisfy equation (4.18), i.e.

$$(u_2)_r = a_2(k_0.\ r, z)u_2 + b_2(k_0, r, z)(u_2)_{zz}. \tag{4.22}$$

Using the first three terms of a Taylor series expansion for u_{m+1} upon u_m, and solving for $(u_2)_{zz}$, we find

$$(u_2)_{zz} = +\frac{2}{h^2}((u_2)^n_{m+1} - u_2) - \frac{2}{h}(u_2)_z. \tag{4.23}$$

Substituting equation (4.23) into equation (4.22) and simplifying, we obtain

$$(u_2)_z = -\frac{h}{2b}(u_2)_r + \frac{h}{2b}a_2 u_2 + \frac{1}{h}((u_2)^n_{m+1} - u_2). \tag{4.24}$$

In matching the conditions on the interface, it should be noted that whereas the wave field u is defined and continuous on the interface, the first derivative and all high order derivatives of u with respect to z are discontinuous at the interface. Thus, in imposing the interface conditions, the limit of the derivatives as they approach the interface from above, or from below, is used.

In view of the first interface condition, equation (4.15), we require that $u_1 = u_2 = u$ in equation (4.21) and (4.24). Substituting the resulting expressions into the second interface condition, equation (4.16), then yields

$$\begin{aligned}
&\rho_2(u_1)_r\left(\cos\Theta - \frac{2b}{h}\sin\Theta\right) + \rho_1(u_2)_r\left(\cos\Theta + \frac{2b}{h}\sin\Theta\right) \\
&\quad = (a_1\rho_2 + a_2\rho_1)u\cos\Theta + \frac{2b\cos\Theta}{h^2}[\rho_1(u_2)^n_{m+1} - (\rho_1 + \rho_2)u + \rho_2(u_1)^n_{m-1}] \\
&\qquad + \frac{2b}{h}(\rho_2 - \rho_1)\frac{u}{v}(v)_r \sin\Theta.
\end{aligned} \tag{4.25}$$

For a horizontal interface, $(u_1)_r = (u_2)_r$, however, for the general case of an irregular interface, a second relationship between $(u_1)_r$ and $(u_2)_r$ is needed. To establish the required relationship, we use a Taylor series expansion of u^{n+1}_{m+1} on u^n_m in medium 1:

$$(u_1)^{n+1}_{m+1} = (u_1 + h(u_1)_z + k(u_1)_r + \tfrac{1}{2}h^2(u_1)_{zz} + \tfrac{1}{2}k^2(u_1)_{rr} + \cdots)^{n+1}_{m+1}. \tag{4.26}$$

Similarly, for medium 2, we obtain

$$(u_2)^{n+1}_{m+1} = (u_2 + h(u_2)_z + k(u_2)_r + \tfrac{1}{2}h^2(u_2)_{zz} + \tfrac{1}{2}k^2(u_2)_{rr} + \cdots)^{n+1}_{m+1}. \tag{4.27}$$

For an arbitrary k, we take

$$h = k\tan\Theta. \tag{4.28}$$

The first interface condition, equation (4.15), implies $(u_1)^{n+1}_{m+1} = (u_2)^{n+1}_{m+1}$. We, thus, equate the r.h.s. of equations (4.26) and (4.27), and again make use of equation (4.15) to obtain

$$(u_1)_r + (u_1)_z\tan\Theta = (u_2)_r + (u_2)_z\tan\Theta. \tag{4.29}$$

Substituting equation (4.21) and (4.24) into equation (4.29), then yields the second relationship

between $(u_1)_r$ and $(u_2)_r$, i.e.

$$(u_1)_r\left(\cos\Theta+\frac{h}{2b}\sin\Theta\right)-(u_2)_r\left(\cos\Theta-\frac{h}{2b}\sin\Theta\right)$$

$$=\frac{h}{2b}(a_1+a_2)u\sin\Theta+\frac{\sin\Theta}{h}[(u_2)^n_{m+1}-2u+(u_1)^n_{m-1}]. \quad (4.30)$$

Equations (4.25) and (4.30) may be solved simultaneously, yielding

$$(u_1)_r=\alpha_1 u_1+\{\beta_1(u_2)^n_{m+1}-(\beta_1+\gamma_1)u_1+\gamma_1(u_1)^n_{m-1}\} \quad (4.31)$$

and

$$(u_2)_r=\alpha_2 u_2+\{\beta_2(u_2)^n_{m+1}-(\beta_2+\gamma_2)u_2+\gamma_2(u_1)^n_{m-1}\}. \quad (4.32)$$

The coefficients in equation (4.31) are given by

$$\alpha_1=\Delta^{-1}\left\{\rho_1 a_2+a_1(\rho_1\sin^2\Theta+\rho_2\cos^2\Theta)+\frac{h}{2b}a_1\sin\Theta\cos\Theta(\rho_1-\rho_2)\right.$$
$$\left.-\left(\cos\Theta-\frac{h}{2b}\sin\Theta\right)\frac{2b}{h}(\rho_1-\rho_2)\frac{v_r}{v}\sin\Theta\right\}, \quad (4.33)$$

$$\beta_1=\Delta^{-1}\frac{2b}{h^2}\rho_1, \quad (4.34)$$

$$\gamma_1=\Delta^{-1}\left\{\frac{2b}{h^2}[(\rho_2\cos^2\Theta+\rho_1\sin^2\Theta)+\frac{1}{h}(\rho_1-\rho_2)\sin\Theta\cos\Theta]\right\}. \quad (4.35)$$

Similarly, in equation (4.32) the coefficients are

$$\alpha_2=\Delta^{-1}\left\{\rho_2 a_1+a_2(\rho_1\sin^2\Theta+\rho_2\cos^2\Theta)+\frac{h}{2b}a_2\sin\Theta\cos\Theta(\rho_1-\rho_2)\right.$$
$$\left.-\left(\cos\Theta-\frac{h}{2h}\sin\Theta\right)\frac{2b}{h}(\rho_1-\rho_2)\frac{v_r}{v}\sin\Theta\right\}, \quad (4.36)$$

$$\beta_2=\Delta^{-1}\left\{\frac{2b}{h^2}\left[(\rho_1\cos^2\Theta+\rho_2\sin^2\Theta)+\frac{1}{h}(\rho_1-\rho_2)\sin\Theta\cos\Theta\right]\right\}, \quad (4.37)$$

$$\gamma_2=\Delta^{-1}\frac{2b}{h^2}\rho_2, \quad (4.38)$$

where

$$\Delta=\left[(\rho_1+\rho_2)+(\rho_{1_1}-\rho_2)\left(\frac{h}{2b}+\frac{2b}{h}\right)\sin\Theta\cos\Theta\right].$$

We now proceed to incorporate the interface equations given by equations (4.31) and (4.32) into an IFD solution of the PE. As shown in Fig. 4.7, u^n_m and u^{n+1}_{m+1} satisfy irregular interface conditions. In expressing range partial derivatives at these two interface points, the points, u^n_{m+1} and u^{n+1}_m below and above the interface are needed to derive a finite difference representation. In doing so, we consider the following.

In medium 1

$$(u_1)^{n+1}_m=\left[u_1+k(u_1)_r+\frac{k^2}{2!}(u_1)_{rr}+\cdots\right]^n_m \quad (4.39)$$

and

$$\frac{\partial(u_1)^{n+1}_m}{\partial r}=\left(\frac{\partial u_1}{\partial r}+k\frac{\partial^2 u_1}{\partial r^2}+\frac{k^2}{2!}\frac{\partial^3 u_1}{\partial r^3}+\cdots\right)^n_m. \quad (4.40)$$

Then, neglecting terms of third order and higher in equation (4.40), we have

$$\frac{k}{2}\frac{\partial (u_1)_m^{n+1}}{\partial r} = \left[\frac{k}{2}\frac{\partial u_1}{\partial r} + \frac{k^2}{2}\frac{\partial^2 u_1}{\partial r^2}\right]_m^n. \tag{4.41}$$

Solving for $\partial^2 (u_1)_m^n / \partial r^2$ in equation (4.41) and substituting the result into equation (4.39) yields

$$(u_1)_m^{n+1} = (u_1)_m^n + \frac{k}{2}\left[\frac{\partial (u_1)_m^n}{\partial r} + \frac{\hat{c}(u_1)_m^{n+1}}{\partial r}\right]. \tag{4.42}$$

Similarly, in medium 2, we obtain

$$(u_2)_{m+1}^{n+1} = (u_2)_{m+1}^n + \frac{k}{2}\left[\frac{\partial (u_2)_{m+1}^n}{\partial r} + \frac{\hat{c}(u_2)_{m+1}^{n+1}}{\partial r}\right]. \tag{4.43}$$

Equations (4.31) and (4.32) supply the finite difference equations for $\partial (u_1)_m^n / \partial r$ and $\partial (u_2)_{m+1}^{n+1} / \partial r$ that are needed in equations (4.42) and (4.43), respectively. In addition, we require a finite difference representation for the range derivative of the field away from the interface. We use a second order central difference operator for u_{zz}. In medium 1, $(u_1)_m^{n+1}$ satisfies the parabolic wave equation,

$$\frac{\partial (u_1)_m^{n+1}}{\partial r} = (a_1)_m^{n+1}(u_1)_m^{n+1} + \frac{b}{h^2}((u_1)_{m+1}^{n+1} - 2(u_1)_m^{n+1} + (u_1)_{m-1}^{n+1}). \tag{4.44}$$

Similarly, in medium 2, $(u_2)_{m+1}^n$ satisfies the PE,

$$\frac{\partial (u_2)_{m+1}^n}{\partial r} = (a_2)_{m+1}^n (u_2)_{m+1}^n + \frac{b}{h^2}((u_2)_{m+2}^n - 2(u_2)_{m+1}^n + (u_2)_m^n). \tag{4.45}$$

We use equation (4.31) for $\partial (u_1)_m^n / \partial r$, and equation (4.44) for $\partial (u_1)_m^{n+1} / \partial r$ in equation (4.42), to obtain our IFD representation in medium 1:

$$\left\{1 - \frac{k}{2}\left((a_1)_m^{n+1} - \frac{2b}{h^2}\right)\right\}(u_1)_m^{n+1} - \frac{1}{2}\frac{kb}{h^2}((u_1)_{m-1}^{n+1} + (u_1)_{m+1}^{n+1})$$

$$= \left\{1 + \frac{k}{2}(\alpha_1 - \beta_1 - \gamma_1)\right\}(u_1)_m^n + \frac{1}{2}k(\gamma_1 (u_1)_{m-1}^n + \beta_1 (u_2)_{m+1}^n). \tag{4.46}$$

Substituting equation (4.32) for $\partial (u_2)_{m+1}^{n+1} / \partial r$, and equation (4.45) for $\partial (u_2)_{m+1}^n / \partial r$ in (4.43) we obtain for medium 2

$$\left\{1 - \frac{k}{2}(\alpha_2 - \beta_2 - \gamma_2)\right\}(u_2)_{m+1}^{n+1} - \frac{1}{2}k(\gamma_2 (u_1)_m^{n+1} + \beta_2 (u_2)_{m+2}^{n+1}).$$

$$= \left\{1 + \frac{k}{2}(a_2)_{m+1}^n - \frac{2b}{h^2}\right\}(u_2)_{m+1}^n + \frac{1}{2}\frac{kb}{h^2}((u_2)_m^n + (u_2)_{m+2}^n). \tag{4.47}$$

4.3.3. Local truncation error

To estimate the local truncation error, we will compare an exact solution of equation (4.11), subject to the interface conditions (4.15) and (4.16), to the finite difference solutions described by equations (4.46) and (4.47). The exact solution for $(u_1)_m^{n+1}$ can be represented by the Taylor series.

$$(u_1)_m^{n+1} = (u_1 + k(u_1)_r + \tfrac{1}{2}k^2(u_1)_{rr} + (k^3/3!)(u_1)_{rrr} + \cdots)_m^n. \tag{4.48}$$

It is easily seen that the Taylor series expansion of $((u_1)_r)_m^{n+1}$ is

$$((u_1)_r)_m^{n+1} = ((u_1)_r + k(u_1)_{rr} + \tfrac{1}{2}k^2(u_1)_{rrr} + \cdots)_m^n. \tag{4.49}$$

Solving equation (4.49) for $(u_1)_{rr}$ and substituting the result into equation (4.48) yields

$$(u_1)_m^{n+1} = (u_1)_m^n + \frac{k}{2}[((u_1)_r)_m^n + ((u_1)_r)_m^{n+1}] - (k^3/12)((u_1)_{rrr})_m^n + \cdots. \tag{4.50}$$

A similar result may be obtained for $(u_2)_{m+1}^{n+1}$,

$$(u_2)_{m+1}^{n+1} = (u_2)_{m+1}^{n} + \frac{1}{2}k\left[((u_2)_r)_{m+1}^{n} + \frac{\partial (u_2)_{m+1}^{n+1}}{\partial r}\right] - (k^3/12)((u_2)_{rrr})_{m+1}^{n} + \cdots. \tag{4.51}$$

Comparing equations (4.50) and (4.51) against equations (4.42) and (4.43) reveals two sources of error: the first is due to the truncation of the Taylor series in the range variable r, the second is due to the finite difference approximations [(4.31), (4.32) and (4.46), (4.47)] used for the derivatives of the field with respect to range variable r. The latter error is the more difficult one to estimate.

We return to equations (4.21) and (4.24), and retain additional terms in the Taylor series to obtain

$$(u_1)_z = \frac{h}{2b}(u_1)_r - \frac{h}{2b}a_1 u_1 + \frac{1}{h}(u_1 - (u_1)_{m-1}^{n}) - \frac{h^2}{3!}(u_1)_{zzz} + \frac{h^3}{4!}\frac{\partial^4 u_1}{\partial z^4} + \cdots \tag{4.52}$$

and

$$(u_2)_z = -\frac{h}{2b}(u_2)_r - \frac{h}{2b}a_2 u_2 + \frac{1}{h}((u_2)_{m+1}^{n} - u_2) - \frac{h^2}{3!}(u_2)_{zzz} + \frac{h^3}{4!}\frac{\partial^4 u_2}{\partial z^4} + \cdots. \tag{4.53}$$

Substituting equations (4.52) and (4.53) into equation (4.16) and applying the first interface condition, equation (4.15), we obtain

$$\rho_2(u_1)_r\left(\cos\Theta - \frac{2b}{h}\sin\Theta\right) + \rho_1(u_2)_r\left(\cos\Theta + \frac{2b}{h}\sin\Theta\right)$$

$$= R_1 + \frac{bh}{3}\cos\Theta\left\{\rho_2(u_1)_{zzz} - \rho_1(u_2)_{zzz} - \frac{h}{4}\left[\rho_2\frac{\partial^4 u_1}{\partial z^4} + \rho_1\frac{\partial^4 u_2}{\partial z^4}\right]\right\} + \cdots, \tag{4.54}$$

where R_1 is the r.h.s. of equation (4.25). Substituting equations (4.52) and (4.53) into equation (4.30) yields a second relationship between $(u_1)_r$ and $(u_2)_r$,

$$(u_1)_r\left(\cos\Theta + \frac{h}{2b}\sin\Theta\right) - (u_2)_r\left(\cos\Theta - \frac{h}{2b}\sin\Theta\right)$$

$$= R_2 + \frac{h^2\sin\Theta}{3!}\left\{(u_1)_{zzz} - (u_2)_{zzz} - \frac{h}{4}\left[\frac{\partial^4 u_1}{\partial z^4} + \frac{\partial^4 u_2}{\partial z^4}\right] + \cdots\right\}, \tag{4.55}$$

where R_2 is the r.h.s. of equation (4.30). If we solve equations (4.54) and (4.55) for $(u_1)_r$ and $(u_2)_r$ and compare the results with those given by equations (4.31) and (4.32), we find that the leading error terms in the finite difference approximations for the range derivatives of the field are given by

$$E[(u_1)_r] = \Delta^{-1}\frac{bh}{3!}(u_1)_{zzz}\left\{(\rho_1+\rho_2) + (\rho_1-\rho_2)\right.$$
$$\left.\times\left[\sin^2\Theta - \cos^2\Theta + \frac{h}{b}\sin\Theta\cos\Theta\right]\right\} - \Delta^{-1}\frac{bh}{3}(u_2)_{zzz}\rho_1 \tag{4.56}$$

and

$$E[(u_2)_r] = \Delta^{-1}\frac{bh}{3}(u_1)_{zzz}\rho_2 - \Delta^{-1}\frac{bh}{3!}(u_2)_{zzz}\left\{(\rho_1+\rho_2) + (\rho_1-\rho_2)\right.$$
$$\left.\times\left[\cos^2\Theta - \sin^2\Theta + \frac{h}{b}\sin\Theta\cos\Theta\right]\right\}. \tag{4.57}$$

From equations (4.56) and (4.57), we see that for points on the interface, the leading error term for the range derivative of the field is of first order in the depth increment h. For all other points, the error in the derivatives of the field is second order in h. Using equations (4.56) and (4.57) in equations (4.50) and (4.51), it may be readily determined that the leading terms in the truncation error are given by

$$E[u_m^{n+1}] = E[u_{m+1}^{n+1}] = O(kh + k^3), \tag{4.58}$$

for points on or adjacent to the interface.

It is seen that from the truncation error estimate that $\lim_{h,k\to 0} k^{-1}E(u)\to 0$, thus establishing the consistency. Since this formulation is incorporated into the IFD model used to solve the PE (4.11), the stability relies on the stability of the IFD model which was addressed by Lee *et al.* [4].

4.4. DISCUSSION

The validity of this model is examined in two ways. First, the interface wave field representation as expressed by equations (4.46) and (4.47) is shown to reduce to results previously obtained for a continuous medium, thus, confirming consistency with the original IFD model. Second, the model is shown to yield numerical results to a selected test problem that are in agreement with the known solution.

The interface model developed in this chapter is based on the PE, equation (4.11). For a continuous ocean medium (having a constant density and continuous sound velocity) the wave field u is assumed to satisfy equation (4.11) everywhere. Hence, the finite difference representation for u_r on the interface must reduce to a finite difference form of equation (4.11) for a continuous medium.

Consider a horizontally stratified ocean as shown in Fig. 4.8. In medium 1, u_1 must satisfy equation (4.11) with $a_1(k_0, r, z) = (ik_0/2)\,([c_0/c_1(r,z)]^2 - 1)$ and an associated density ρ_1. Similarly, in medium 2, u_2 must satisfy equation (4.11) with an associated sound speed c_2 and density ρ_2. At the interface, the range derivative of the wave field has the finite difference representation given by equations (4.31) and (4.32) in medium 1 and medium 2, respectively. For a horizontal interface, $\Theta = 0$, and

$$(u_1)_r = (u_2)_r = u_r$$
$$= (\rho_1+\rho_2)^{-1}\left\{[\rho_1 a_2 + \rho_2 a_1]u + \frac{2b}{h^2}[\rho_1 u^n_{m+1} - (\rho_1+\rho_2)u^n_m + \rho_2 u^n_{m-1}]\right\}, \tag{4.59}$$

in agreement with the results obtained for a horizontal interface by McDaniel and Lee [5]. For a continuous ocean medium, $\rho_1 = \rho_2$ and $c_1 = c_2$ at the interface, equation (4.59) reduces to

$$u_r = au + \frac{b}{h^2}[u^n_{m+1} - 2u^n_m + u^n_{m-1}]. \tag{4.60}$$

Regarding $h^{-2}[u^n_{m+1} - 2u^n_m + u^n_{m-1}]$ as a central difference for u_{zz}, equation (4.60) is a difference equation of equation (4.11), establishing the validity.

Next, we consider the range-independent environment shown in Fig. 4.9 for which the transmission loss may be readily computed using normal-mode theory. A source of 100 Hz frequency is placed at a depth of 30 m below the water surface; the receiver is at a depth of 90 m. A single interface is present demarcating the boundary between water and sediment at a depth of 240 m. The density of the water is 1.0 g/cm^3 and the density of the sediment is 2.1 g/cm^3. The sound-speed profile (Fig. 4.9) contains two linear segments in the upper water column and is constant at 1505 m/s in the sediment.

A normal-mode model was used to calculate the transmission loss out to a maximum range of 2 km. This normal-mode model treats the lower medium as semi-infinite and treats the interface correctly. Hence, this normal-mode solution is used as a reference solution for comparison. To

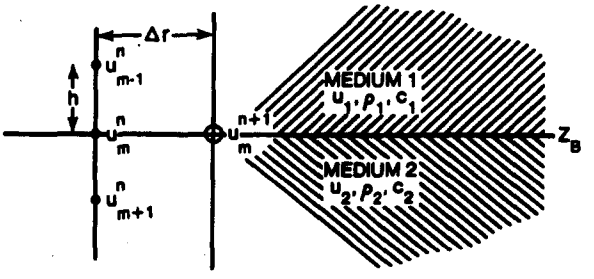

Fig. 4.8. The horizontal interference between two media.

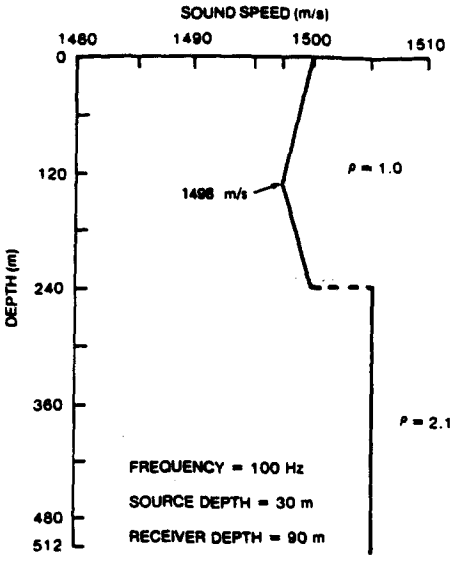

Fig. 4.9. Sound-speed profile.

verify the importance of correctly modeling the wave field on the interface, the transmission loss was first calculated using the IFD model but neglecting the density discontinuity at the water–sediment interface. As is evident in Fig. 4.10, this computation displays poor agreement with the normal-mode solution. When, however, the interface conditions are incorporated into the IFD model, the resulting solution is in excellent agreement with the normal-mode result as shown in Fig. 4.10.

To further illustrate the utility of this model, we consider acoustic propagation from deep to shallow water in a realistic ocean environment [6, 7]. The environment, shown in Fig. 4.11, consists of two range-independent regions joined by a region in which the water depth and bottom properties change linearly with range. Medium 1 is water of density 1.0 g/cm^3 and medium 2 is a sediment having a density of 1.7 gm/cm^3. (The deeper sediment layers have no effect on acoustic propagation at the source frequency of 100 Hz.) For source and receiver depths of 50 and 73 m, respectively, a correct treatment of boundary interaction in the transition region was found to be essential to predicting transmission losses in shallow water.

This problem was treated comprehensively by McDaniel [8] using coupled-mode theory. We will, hence, employ the mode-coupling result as a reference solution. Using the IFD model with the interface wave field representation developed in this paper, transmission losses were computed to

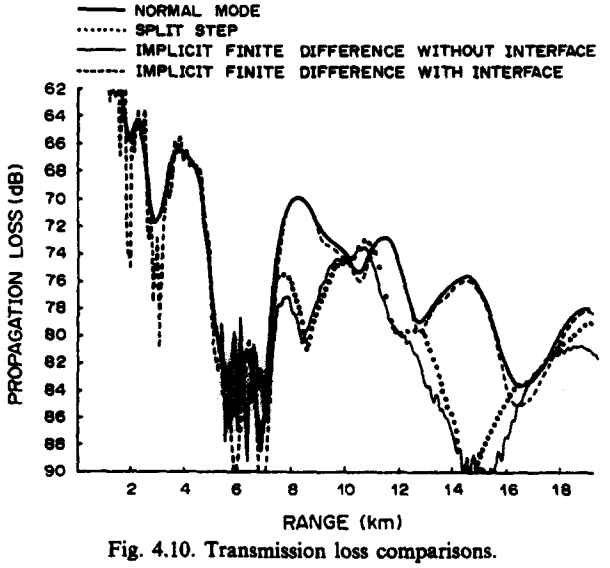

Fig. 4.10. Transmission loss comparisons.

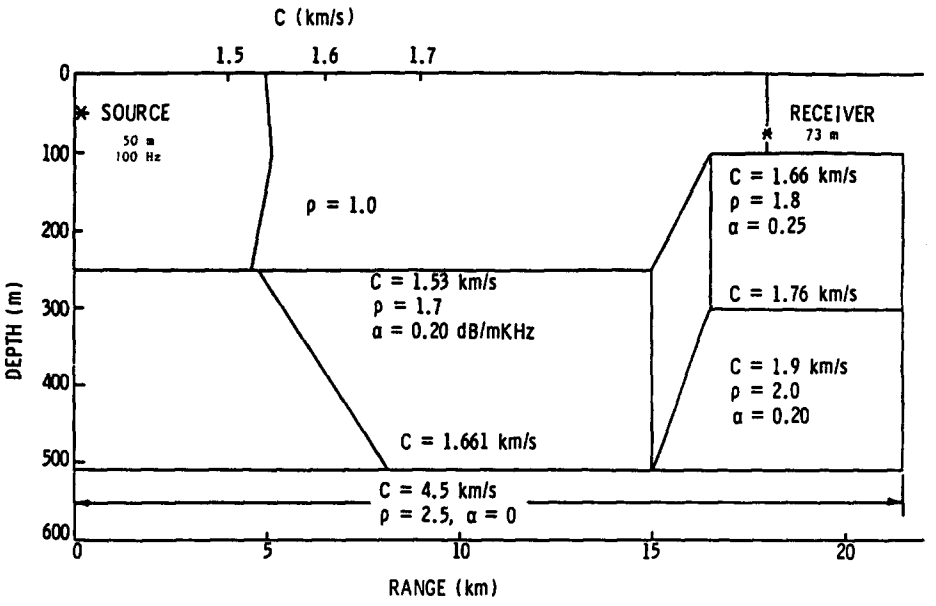

Fig. 4.11. Example environment.

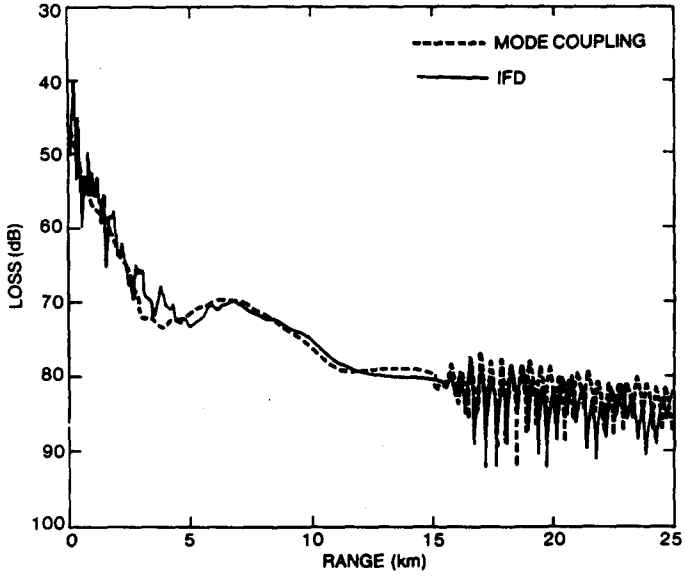

Fig. 4.12. Range-dependent model comparison.

a maximum range of 25 km. In Fig. 4.12, the results obtained are shown to be in excellent agreement with the mode-coupling solution.

A mathematical model based on the parabolic approximation to the acoustic wave equation that accurately treats the wave field at the interface between different media is introduced. This model extends the applicability of the PE to ocean environments where strong interaction with the seabed occurs. This model may be used to treat the acoustic field, not only at the water–sediment interface, but also at interfaces between deeper sedimentary strata.

REFERENCES

1. F. D. Tappert, The parabolic approximation method. In *Wave Propagation and Underwater Acoustics* (Eds J. B. Keller and J. S. Papadakis); *Lecture Notes in Physics*, Vol. 70. Springer, Berlin (1977).
2. F. R. DiNapoli and R. L. Deavenport, Numerical models of underwater acoustic propagation. In *Topics in Current Physics* (Ed. J. A. DeSanto). Springer, Berlin (1979).

3. B. Carnahan, H. A. Luther and J. O. Wikes, In *Applied Numerical Methods*. Wiley, New York (1969).
4. D. Lee, G. Botseas and J. S. Papadakis, Finite-difference solution to the parabolic wave equation. *J. acoust. Soc. Am.* **70** (8), 795–800 (1981).
5. S. T. McDaniel and D. Lee, A finite-difference treatment of interface conditions for the parabolic wave equation: the horizontal interface. *J. acoust. Soc. Am.* **71** (4), 855–858 (1982).
6. D. Lee and S. T. McDaniel, A finite-difference treatment of interface conditions for the parabolic wave equation: the irregular interface. *J. acoust. Soc. Am.* **73** (5), 1441–1447 (1983).
7. D. Lee and S. T. McDaniel, Wave field computations on the interface: an ocean acoustic model. *Math. Model.* **4**, 471–488 (1983).
8. S. T. McDaniel, Mode-coupling due to interaction with the seabed. *J. acoust. Soc. Am.* **72** (3), 916–923 (1982).